Int. J. Multiphase Flow. Vol. 4, pp. 65–79. Pergamon/Elsevier. 1978. Printed in Great Britain.

# TWO-PHASE REACTIVE PARTICLE FLOW THROUGH NORMAL SHOCK WAVES

HERMAN KRIER and AMIR MOZAFFARIAN
University of Illinois at Urbana-Champaign, Urbana, IL 61801, U.S.A.

(*Received* 2 *June* 1977)

**Abstract**—An analysis is presented for the steady one-dimensional flow behind a normal shock wave of a compressible gas containing small spherical particles of solid propellant. The solids mass fraction is assumed large enough to require that the void volume fraction be retained as a variable in the governing conservation equations. The particles are ignited by the shocked air and by viscous interaction. Propellant gases are then generated which depend on the instantaneous size of the particles and on the linear burning rate. The latter is assumed dependent upon the local pressure and the particle temperature. These calculations are of interest because of the potential hazards of such particle flows, in that extreme pressures are predicted within the relaxation zone, pressures even greater than those calculated for the final equilibrium conditions. The results stress the importance of the Mach number of the normal (strong shock) and the energy content of the propellant (J/kg).

## 1. INTRODUCTION

The steady flow of suspensions of particles in compressible gases with the possible existence of shock waves has been analyzed by previous investigators, generally for inert particles in air. The work of Carrier (1958), Rudinger (1964, 1965), Marble (1963), and Kriebel (1964) represent the foundation developed in this area. The significant calculation is generally the relaxation zone structure and length behind normal shock waves which have generated velocity and temperature differences of the particle and gas phases.

Modifications of the normal shock analysis for a mixture of liquid droplets in the air have been carried out by Lu & Chiu (1966), Panton & Oppenheim (1968) and Narkis & Gal-or (1975). The majority of all these investigators assumed in their models that the particle (or liquid) volume was negligible compared to the volume of the air (gas) stream. Such an assumption greatly simplifies the solution to the models, and may even be a necessary requirement to truly allow for "strong" shock (two-phase) waves in a laminar flow regime. Excellent reviews on the subject of the possibility of "strong" and "weak" (diffusive) shock in two phase mixtures are given by Wallis (1969) and Rudinger (1969).

The work presented here gives the important steps for the analysis of the steady one-dimensional flow through a normal shock wave of compressible gases containing solid propellant. A model is developed for particles assumed to be propellant, which after being ignited in the relaxation zone from the heat transferred by the shocked (high temperature) air and viscous interaction, begin to burn at rates dependent upon both the local pressure and the particle temperature. The solid volume fraction is *not* assumed to be zero. Each step of the modeling procedure is developed with sufficient detail so that the equations in their final form can be understood as to their physical importance.

### *Previous related work*

Carrier (1958) analyzed the plane steady decelerated flow of gas heavily laden with particles by eliminating one of the variables ($z$, the space-coordinate) between the two lag equations. Kriebel (1964) gave an approximate analytical solution for weak shock waves and computer results for strong shocks where three particle sizes were present. Almost simultaneously, but independently, Rudinger (1964, 1965) studied the numerical case for solid particles where he varied shock strengths, drag coefficients and heat-transfer correlations. He noted that the velocities and temperatures did not always change monotonically toward their equilibrium

values. Investigators who took into account the mass transfer between the phases were Lu & Chiu (1966) and Panton & Oppenheim (1968), who studied the structure of the relaxation zone where the particles were liquid droplets, and Narkis & Gal-or (1975).

More recently Kuo & Summerfield (1974, 1975) considered the combustion of solid propellant particles through a discontinuous wave structure. However their work considered only a "weak" shock wave structure. That is, the Mach number of the gas is less than unity, but the Mach number of the "mixture" is greater than unity. The solids loading (volume fraction) was very large, but turbulent fluid interchange was only "accounted" for in the viscous drag (which causes the pressure drop) and the heat-transfer coefficient. Also, the initialized stimulus for particle ignition is produced by an external source, which unfortunately was not represented in any of the equations expressed in both papers by Kuo & Summerfield (1974, 1975).

The model developed here is applied to both strong and weak shock waves. No external source is required to ignite the particles. The jump conditions are derived which determine the final fluid properties at the end of the long relaxation zone. The work also shows that the drag relations and heat-transfer correlations one assumes can dominate the wave structure and prediction of ignition. The application of the work, especially for the strong shock waves, is that of predicting a potential hazards problem in particle dust mixtures. Such an extension for dust mixtures of a solid fuel (not propellant) would, of course, require a solution to the air and fuel vapor species conservation equations as well as the ones shown here.

## 2. PROBLEM OF INTEREST AND FORMULATION OF GOVERNING EQUATIONS

In this section the theoretical model of steady state state strong shock wave initiation of particulate propellant or explosives is discussed. The assumptions which apply here and the required conservation equations which must be satisfied are presented below.

Initially the two phases are in total equilibrium at some velocity $U_p = U_g = V_o$, temperature $T_p = T_g = T_o$ and pressure $P_o$, where $U$ is the velocity with respect to laboratory coordinates, $V$ is the shock wave velocity, subscript $p$ refers to particle properties and $g$ refers to gas properties. A strong shock wave with constant velocity $V_o$ propagating through the mixture will upset the equilibrium between the two phases. As depicted in figure 1 (for inert particles) in this nonequilibrium region the gas and the particle velocities drop whereas the gas temperature rises (as a result of friction due to the differences in phase velocities). Particles now find themselves in a high temperature surroundings and their temperature rises according to heat transfer laws. At a location downstream, the particle temperature reaches its ignition value, $T_{ign}$. The distance between the origin of the coordinate axis, $Z$, and the location where the particle ignition occurs is called, $Z_{cw}$, combustion front distance. Chemical reaction occurs until the particles burn out, i.e.

$$Z_{cw} \leqslant Z \leqslant Z_\infty,$$

where $Z_\infty$ is the distance at which particles burn out (i.e. the final equilibrium state where $\epsilon = 1$). Hence $Z_\infty$ is the thickness of the relaxation zone.

*Assumptions*

It is assumed that, (a) the gas is treated as a continuum of a generally ideal, perfect gas. At high pressures a co-volume correction is inserted into the state equation. (b) The gas alone is inviscid except for the interaction with the particles and the dissipation in the discontinuous shock front. (c) The particles are assumed to be incompressible; i.e. $\rho_p$ = constant. (d) Transport properties of the gas and the particles are appropriate averages and held constant. (e) The particles are of spherical shape because of the availability of well established empirical heat transfer and drag equations. (f) The particles are uniformly distributed in the gas. (g) The

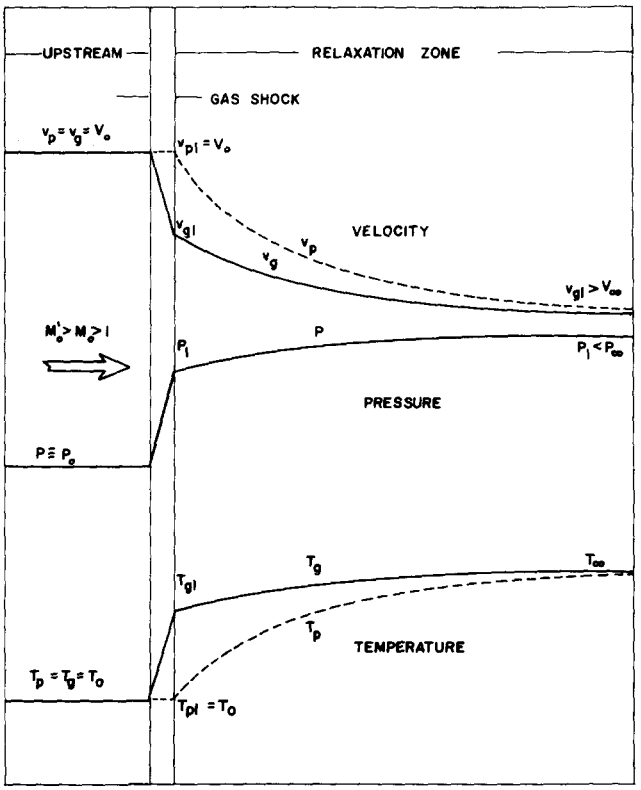


Figure 1. Typical pressure, velocity and temperature variations through a "strong" two-phase flow shock wave (inert particles).

particles have a sufficiently large thermal conductivity relative to the gas so that their internal temperature is uniform. This approximation allows the use of one specific temperature to define the solid phase. Rudinger (1969) has presented a discussion regarding the limiting particle size and thermal resistance which validates this approximation. (h) Energy exchange between the particles and the gas occurs only through convection (i.e. radiation transport has been neglected). (i) There are no mass, momentum and energy losses from the system (i.e. the mixture). (j) The particles and the gas are in velocity and temperature equilibrium upstream and again far downstream of the shock wave. (This, of course, means the shock wave moves into a quiescent mixture of uniformly dispersed particles in air.) (k) The body forces, especially gravity, are neglected. (l) One dimensional flow is assumed throughout; turbulent flow fluctuations are neglected. (m) The structure of the shock wave is not affected by the presence of the solid phase so that the gas state variables after the shock are found from the classical shock wave solutions. (n) The particle temperature is assumed to be constant across the shock wave since the thickness of the shock wave is small compared to the particle size. (o) However, particle velocity across the shock wave changes somewhat since they receive an impulse. (p) The burning rate of the particles is pressure sensitive and also affected by changes in particle temperature. A steady-state burning rate equation, assumed known, is used. (q) The propellant gases are assumed to be identical to that of air, and they mix instantaneously with the air.

*General conservation equations*

The one-dimensional form of the unsteady conservation equations are expressed below. This formulation utilizes the concept of a "separated" two-phase flow, as defined in the text by Wallis (1969). A different form for the mixture or field balance equations arise if one assumes a "continuum" two-phase, as defined by Soo (1967) and used by Krier & Van Tassell (1975). However, it can be shown that both concepts are approximately identical when the solids

loading, $(1-\epsilon)$ is near unity, $\epsilon$ is the gas void fraction and for cases when the gas and solid velocity are of the same order. Thus we express the following:
Gas continuity:

$$\frac{\partial}{\partial t}(\epsilon\rho_g)+\frac{\partial}{\partial z}(\epsilon\rho_g U_g)=\Gamma_g, \tag{1}$$

where $\Gamma_g$ is the rate of production of gas.
Particle continuity:

$$\frac{\partial}{\partial t}[(1-\epsilon)\rho_p]+\frac{\partial}{\partial z}[(1-\epsilon)\rho_p U_p]=-\Gamma_g. \tag{2}$$

Mixture momentum:

$$\frac{\partial}{\partial t}[\epsilon\rho_g U_g+(1-\epsilon)\rho_p U_p]+\frac{\partial}{\partial z}[\epsilon\rho_g U_g^2+(1-\epsilon)\rho_p U_p^2]=-\frac{\partial}{\partial z}P_g-\frac{\partial}{\partial z}[(1-\epsilon)\tau_p], \tag{3}$$

where $\tau_p$ is the particle–particle stress.
Mixture energy:

$$\frac{\partial}{\partial t}[\epsilon\rho_g e_{g_o}+(1-\epsilon)\rho_p e_{p_o}]+\frac{\partial}{\partial z}[\epsilon\rho_g U_{g_o}+(1-\epsilon)\ {}_pU_p e_{p_o}]+\frac{\partial}{\partial z}[\epsilon P_g U_g+(1-\epsilon)P_g U_g]$$
$$+\frac{\partial}{\partial z}[(1-\epsilon)\tau_p U_p]=0. \tag{4}$$

Hence

$$e_{g_o}\equiv C_{v_g}T_g+1/2U_g^2, \tag{4a}$$

$$\epsilon_{p_o}\equiv C_pT_p+1/2U_p^2+E_f \tag{4b}$$

when $e_{g_o}$ is the stagnation energy of the gas, $e_{p_o}$ is the stagnation energy of the solid phase, $E_f$ is the energy of reaction.
Gas equation of state:

$$P_g(\rho_g^{-1}-b)=\mathcal{R}_gT_g. \tag{5}$$

Particle force balance:

$$\left[\frac{\pi}{6}d_p^3\right]\rho_p\frac{D_pU_p}{Dt}=C_D\left[\frac{\pi}{4}d_p^2\right]1/2\rho_g(U_g-U_p)|U_g-U_p|. \tag{6}$$

Particle energy balance:

$$\left[\frac{\pi}{6}d_p^3\right]\rho_pC_p\frac{D_pT_p}{Dt}=(\pi d_p^2)\frac{N_uk_g}{d_p}(T_g-T_p)-\left(\frac{\pi}{6}d_p^3\right)\Gamma_gh_{fg}, \tag{7}$$

where $N_u$ is the Nusselt number, $k_g$ is the gas thermal conductivity, $d_p$ is the particle diameter. The last term in the R.H.S. of [7] is inserted to account for latent heat of sublimination, $h_{fg}$, which is nonzero only after ignition.

Conversely one may drop the last term in [7] and instead assume that the Nusselt number

$Nu$ is reduced after burning commences, because of "blowing" into the thermal boundary layer around the particle. Of course, the proper Nusselt number variation is actually unknown, and is an independent study in itself.

In order to obtain the steady-state structure of the chemically reacting particle laden shocks, the coordinate system is taken to travel at the same velocity as the shock wave. The required transformation can simply be,

$$\beta \equiv V_o t - Z, \tag{8}$$

$$\tau \equiv t \tag{9}$$

where $\beta$ is the transformed space coordinate, $V_o$ is the speed of propagation wave (constant), $\tau$ is the transformed time coordinate. Hence, one can easily obtain

$$v_g(\beta) \equiv V_o - U_g(Z), \tag{10}$$

$$v_p(\beta) \equiv V_o - U_p(Z), \tag{11}$$

where $v_g$ is the gas velocity seen by an observer fixed on shock wave, and $v_p$ is the particle velocity seen by an observer fixed on shock wave. Neglecting shear forces and particle collisions (i.e. $\tau_p = 0$) and all time derivatives, the transformed governing equations [1]–[4], [6] and [7] will change to six simpler ordinary differential equations; namely,
Gas continuity:

$$\frac{d}{d\beta}[\epsilon\rho_g v_g] = \Gamma_g. \tag{12}$$

Particle continuity:

$$\frac{d}{d\beta}[(1-\epsilon)\rho_p v_p] = -\Gamma_g. \tag{13}$$

Mixture momentum:

$$\frac{d}{d\beta}[\epsilon\rho_g v_g^2 + (1-\epsilon)\rho_p v_p^2] = -\frac{dP_g}{d\beta}. \tag{14}$$†

Mixture energy:

$$\frac{d}{d\beta}[\epsilon\rho_g v_g e_{g_o} + (1-\epsilon)\rho_p v_p e_{p_o}] = -\frac{d}{d\beta}[\epsilon v_g P_g + (1-\epsilon)v_p P_g]. \tag{15}$$†

Particle force balance:

$$\rho_p v_p \frac{dv_p}{d\beta} = \frac{3}{4}\frac{C_D}{d_p}\rho_g |v_g - v_p|(v_g - v_p), \tag{16}$$

when $C_D$ is the dry coefficient.
Particle energy balance:

$$\rho_p C_p v_p \frac{dT_p}{d\beta} = 6\frac{N_u k_g}{d_p^2}(T_g - T_p) - \Gamma_g h_{fg}, \tag{17}$$

where $d_p = 2R_p$.

†Note that [14] and [15] can be integrated immediately and the constants evaluated from the initial conditions.

Equations [12]–[17] are expressed in conservation form. In order to solve for each parameter explicitly, i.e. in operator form, a great deal of substitution and algebraic manipulations are required. Here $\Gamma_g = 3(1-\epsilon)r_b/R_p$ after the particles have reached their ignition temperature, where $r_b$ is the burning rate and $R_p$ is the particle radius.

Finally, in the differential operator form of the unknowns, the following relations are derived.

$$\frac{dv_p}{d\beta} = Y_1, \tag{18}$$

$$\frac{dT_p}{d\beta} = Y_2, \tag{19}$$

$$\frac{d\epsilon}{d\beta} = Y_3, \tag{20}$$

$$\frac{dv_g}{d\beta} = \{Y_4^2 Y_7 Y_8 Y_{10} - Y_4(Y_9 + Y_5 Y_8)\}/Y_{11}, \tag{21}$$

$$\frac{dT_g}{d\beta} = \{Y_4 Y_{10}(Y_6 Y_9 - Y_7) + (Y_5 - Y_9)\}/Y_{11}, \tag{22}$$

$$\frac{dP_g}{d\beta} = \{Y_4 Y_6(Y_5 Y_8 + Y_9) - Y_4 Y_7(1 + Y_8)\}/Y_{11}, \tag{23}$$

where,

$$Y_1 = \frac{3}{8}\frac{C_D}{R_p}\frac{\rho_g}{\rho_p}|v_g - v_p|\left(\frac{v_g - v_p}{v_p}\right), \tag{24a}$$

$$Y_2 = \frac{3}{2}\frac{N_u}{R_p^2}\frac{k_g}{\rho_p C_p}\left(\frac{T_g - T_p}{v_p}\right) - \Gamma_g h_{fg}/(\rho_p C_p V_p), \tag{24b}$$

$$Y_3 = \frac{1-\epsilon}{v_p}\left(Y_1 + \frac{3r_b}{R_p}\right), \tag{24c}$$

$$Y_4 = \frac{v_g \rho_g \mathcal{R}_g}{P_g}, \tag{24d}$$

$$Y_5 = \frac{1}{\epsilon}\left[\frac{3(1-\epsilon)}{R_p}\frac{\rho_g}{\rho_p} r_b - v_g Y_3\right], \tag{24e}$$

$$Y_6 = \epsilon \rho_g v_g, \tag{24f}$$

$$Y_7 = 3\frac{\rho_p r_b}{R_p}(1-\epsilon)(v_p - v_g) - (1-\epsilon)\rho_p v_p Y_1, \tag{24g}$$

$$Y_8 = \frac{C_{Vg}}{\mathcal{R}_g}, \tag{24h}$$

$$Y_9 = -\frac{1}{\epsilon}[(1-\epsilon)Y_1 + (v_g - v_p)Y_3] - \left(\frac{1-\epsilon}{\epsilon}\right)\frac{\rho_p C_p v_p Y_2}{P_g} + \left(\frac{1-\epsilon}{\epsilon}\right)\frac{3\rho_p r_b}{R_p P_g}[(v_g - v_p)v_g + (e_{p_o} - e_{g_o})], \tag{24i}$$

$$Y_{10} = \frac{T_g}{P_g}, \tag{24j}$$

$$Y_{11} = Y_4^2 Y_6 Y_8 Y_{10} - Y_4(1 + Y_8). \tag{24k}$$

The six ordinary differential equations [18]–[23] plus the algebraic equation of state [5]

completes the system of seven equations in seven unknowns describing the detailed structure of a steady state chemically reacting particle-laden shock wave. A brief discussion of the method of solution to the above system of equations is presented below.

*Numerical integration scheme*

Numerical integration of the set of first order, coupled, ordinary differential equations [18]–[23], is performed per one step of length, $H$, using a routine called DIFSUB developed by Gear (1971). The interval $H$ may be specified by the user, but features an automatic step size selection, which allows the integrator to take the longest step possible, while satisfying the prescribed error criterion. Either an Adams method or methods suitable for stiff equations can be selected. The starting procedure is automatic and the information retained by DIFSUB about previous steps is stored in such a way to make interpolation to a non-mesh point straightforward.

*Boundary conditions*

For this initial value problem the boundary conditions specified at the equilibrium (cold) end are simply,

$$P = P_o; \quad T_p = T_g = T_o; \quad V_p = V_g = V_o. \tag{25}$$

The state equation gives $\rho_{g_o}$. The solid density, $\rho_{p_o}$ remains an assumed constant. For weak (diffusive) shocks, the solution to [18]–[23] are solved using the conditions specified in relations [25]; although some perturbation in either velocity or temperature is required to start the problem.

For the strong shock ($M_o \equiv V_o/A_o > 1$) the gas is shocked to a greater temperature, $T_{g_1}$, a higher pressure, $P_{g_1}$, and a lower velocity, $V_{g_1}$. Rudinger (1969) has presented the relations for $P_{g_1}/P_0$, $T_{g_1}/V_0$, as well as $M_{g_1}/M_0$. These relations depend only upon $M_0$ and $\gamma_g$ the gas phase specific heat ratio. Here, $A_0$ is the speed of sound of the gas. Thus specification of the conditions [25] immediately determine conditions across the normal shock. These conditions are then the initial values required to begin integration.

The equations are integrated until total relaxation of velocity and temperature has been completed. Appendix A presents the "jump" conservation relation which determines those hot end conditions, namely, $T_g = T_\infty$, $P = P_\infty$, $V_g = V_\infty$. Of course we assume that $\epsilon \to 1$ since $R_p \to 0$ at burnout.

*Additional functional inputs*

(a) *Particle radius.* The particle radius can be calculated from the "Number Density" or simply from the known variation of $\epsilon$. For steady flow it is easy to show that

$$\frac{R_p}{R_{p_o}} = \left(\frac{W_p}{W_{p_o}}\right)^{1/3}, \tag{26}$$

where:

$$W_p = \rho_p A_p U_p, \tag{27a}$$

$$W_{p_o} = \rho_{p_o} A_{p_o} U_{p_o}. \tag{28a}$$

where $A_p$ represents the cross sectional area for the particle flow.

But,

$$\frac{W_p}{A} = \rho_p (1 - \epsilon) U_p, \tag{27b}$$

and

$$\frac{W_{p_a}}{A} = \rho_{p_o}(1-\epsilon_o)U_{p_o}. \qquad [28b]$$

where $A$ represents the total flow area.
Assuming that solid phase density is constant, by appropriate substitutions one can then show that

$$R_p = R_{p_o}\left(\frac{1-\epsilon}{1-\epsilon_o}\frac{U_p}{U_{p_o}}\right)^{1/3}. \qquad [29]$$

(c) *Burning rate.* The usual pressure-dominant propellant burning was assumed to be

$$r_b = a(T_p/T_{p_o})\cdot P^n \qquad [30]$$

where the parameters $a$ and $n$ are assumed known constants.

(c) *Interaction coefficients.* A simple momentum balance, when assuming that the solids volume fraction is negligible gives

$$\frac{\pi}{6}d_p^3\rho_p\frac{\mathrm{D}_p U_p}{\mathrm{D}t} = 3\pi\mu_g d_p(U_g - U_p) \equiv \text{Stoke's drag law.} \qquad [31]$$

In general, Stoke's drag is only accurate if the particle velocity with respect to the gas velocity is small. Thus the R.H.S. of [31] should be replaced by definition of drag. In terms of a drag-coefficient,

$$\frac{\mathrm{D}_p U_p}{\mathrm{D}t} = \frac{3}{4}C_D\frac{\rho_g}{d_p\rho_p}|U_g - U_p|(U_g - U_p). \qquad [32]$$

Since the particle Reynolds number may not be small and hence the Stoke's drag regime would not apply, a more satisfactory drag coefficient was chosen. A "standard" drag coefficient, given by Rudinger (1969) was assumed to be,

$$C_D = 0.48 + \frac{28}{(R_{ep})^{.85}}, \qquad [33a]$$

where the Reynold's number,

$$R_{ep} = \frac{\rho_g d_p|U_g - U_p|\epsilon}{\mu_g}. \qquad [33b]$$

The non-dimensional heat-transfer coefficient, i.e. the Nusselt number was assumed to be of the form

$$N_u = 2 + 0.6P_r^{1/3}Re_p^{1/2} \qquad [34]$$

where, $P_r$ = Prandtl number of the gas = $(\mu_g C_{p_g})/k_g$. Rudinger (1964) has studied the effects of various forms of $C_D$ and $N_u$ as they alter the velocity and temperature variations in the relaxation zone.

(d) *Propellant ignition criterion.* As discussed in the list of assumptions, having assumed that the particles are always at an average uniform temperature, the ignition criterion must simply state that a critical temperature must be reached, at which point the total surface begins

to burn at the rate given by [30]. This ignition temperature rise is typically 10°C to 20°C. Such relatively low temperature increases reflect the use of a bulk solid temperature to represent ignition conditions. This ignition criterion is given support by the work of Derr & Fleming (1973) who showed a strong correlation of a critical temperature and burn rate.

If one assumes instead that there are significant temperature gradients in the solid, as Kuo & Summerfield (1974, 1975) have done, then ignition will begin only if a *surface* temperature exceeds a critical value, usually much larger than the bulk ignition temperature. But to use a propellant surface temperature requires solving the unsteady heat conduction for the particles at every location. This additional equation then replaces the solid particle energy balance, [17], an approach which is unacceptable to us, mainly because the mixture energy equation in the form given in [4] or [5] must be satisfied as presented.

Typical input parameters and other properties of the gas and solid are given in table 1.

Table 1. Typical input parameters

| | |
|---|---|
| Equilibrium conditions at the cold end | |
| $M_o = 2.5$ | |
| $P_o = 1$ [atm] = 1.013 nts/m$^2$) | |
| $T_o = 295$ [K] | $\rho_{g_o} = 1.059$ [kg/m$^3$] |
| $\epsilon_o = 0.95$ | |
| $d_{p_o} = 150$ [$\mu$m] | |
| Thermodynamic gas properties | |
| $k_g = 2.5 \times 10^{-2}$ [W/m K], | $\mu_g = 2.00 \times 10^{-5}$ [kg/m sec] |
| $C_{v_g} = 7.18 \times 10^2$ [J/kg K], | $\gamma_g = 1.4$ |
| $C_p = 1.00 \times 10^3$ [J/kg K], | $MW = 26$ [g/g-mole] |
| Propellant properties | |
| $\rho_p = 1441$ [kg/m$^3$], | $\Delta T_{ign} = 10$°C |
| $E_f = 1.86$ [MJ/kg], | $n = 0.9$ |
| | $a = 0.94 \times 10^{-6} \frac{\text{[cm/sec]}}{(\text{nt/m}^2)^n}$ |

## 3. RESULTS

The structure of the relaxation zone for moderate size solid propellant particles which can burn is presented in figures 2–4, for a propellant assumed to have an energy content of 2.09 MJ/kg and requiring a heat of sublimation at pyrolysis of 0.116 MJ/kg. The initial gas void fraction is $\epsilon_o = 0.95$ giving $m_{p_o} = 72$. All other properties are listed in table 1. Here

$$m_{p_o} = \left[\frac{W_p}{W_g}\right]_o = \frac{(1-\epsilon_o)\rho_p}{\epsilon_o \rho_{g_o}}. \qquad [35]$$

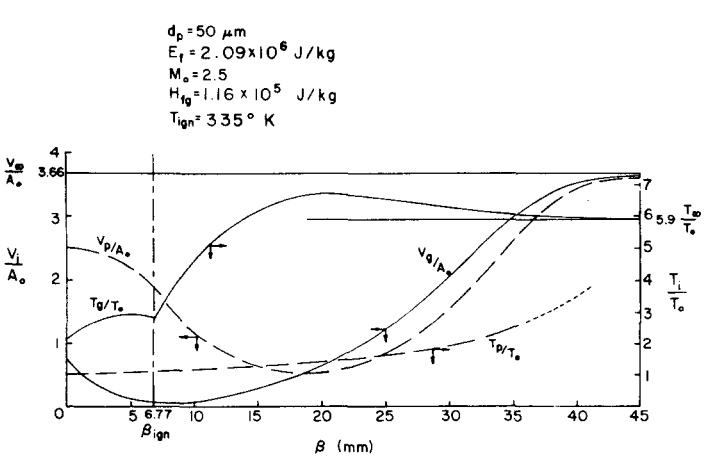


Figure 2. Predictions of the velocities and temperatures behind a strong shock wave of (reactive) solid propellant particles ($d_p = 50$ $\mu$m; $M_o = 2.5$).

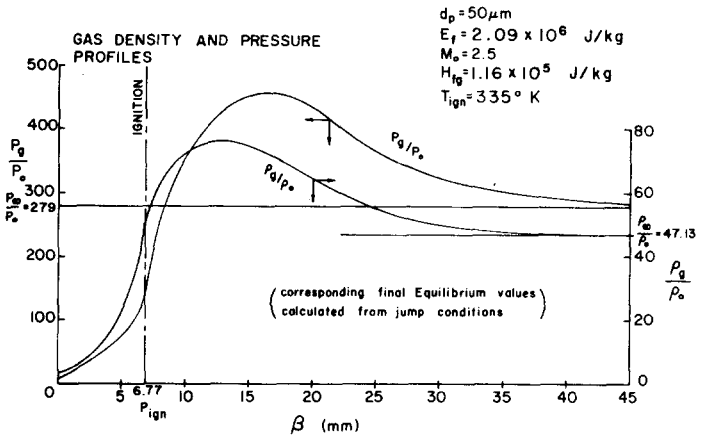


Figure 3. Predictions of the gas density and pressure variation behind a strong shock wave of (reactive) solid propellant particles ($d_p = 50\ \mu m$; $M_o = 2.5$).

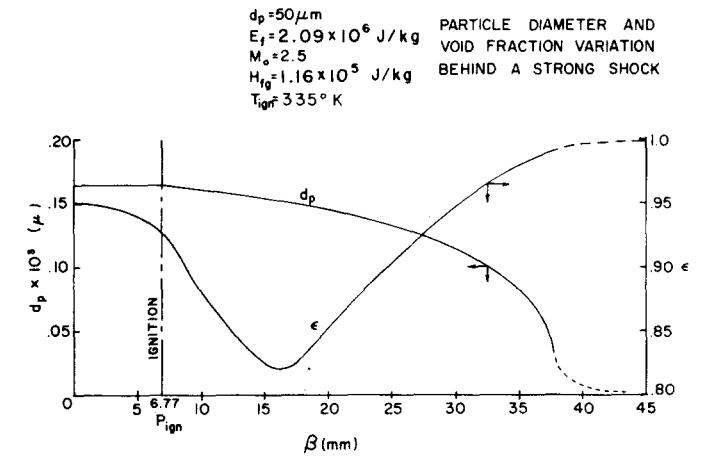


Figure 4. Predictions of the solid propellant size (diameter) and void fraction, $\epsilon$, behind a strong shock wave ($d_p = 50\ \mu m$; $M_o = 2.5$).

Thus, for every gram of air in the mixture, one has 72 g of propellant, which takes up only 5% of the volume.

The velocities are normalized with the sound speed of the (cold) equilibrium mixture, $A_o$. The shock of $M_o = 2.5$ reduces the gas velocity to 0.30 of its initial value, i.e. $V_{g_1}/V_{g_o} = 0.30$ and the subsonic Mach number is $M_1 = 0.513$. Therefore, the initial value of figure 2, for $V_{g_1}/A_o$ at $\beta = 0$ is given by,

$$V_{g_1}/A_o = M_1 \cdot (A_1/A_o) = M_1 \cdot \sqrt{(T_{g_1}/T_0)}. \qquad [36]$$

Since, for $\gamma = 1.4$, $T_{g_1}/T_o = 2.1375$, then by [36], $V_{g_1}/A_o = 0.750$, as shown.

As figure 2 shows, the relaxation zone structure includes a short region, before ignition, in which the velocities and temperatures vary as they would for an inert mixture. At $\beta = Z_{cw}$ (combustion wave) of 6.77 mm the particles have raised their temperature by at least 10 K and begin to burn. The gas temperature immediately increases because of the hot combustion products to a peak value of $T_g/T_o = 6.78$, eventually relaxing to a value of 5.95. Because of the mass source term the gas velocity eventually begins to increase. At the end of the relaxation zone $V_{g\infty}/A_o = 3.66$ which satisfies the end "jump" condition. The relaxation zone thickness will be determined by the particle burnout location, shown in figure 4. The key result is, of course,

that, because of combustion the total relaxation zone is typically an order of magnitude shorter than for an inert mixture under the same condition.

The gas pressure and density variation are shown in figure 3. Notice that the pressure has peaked, at $\beta = 16$ mm, to 462 atm; at the end of the relaxation zone the pressure is still a high value of 279 atm.

Variations of void fraction and particle diameter are shown in figure 4. Notice first the compaction of the solids, reaching a minimum gas void fraction of $\epsilon = 0.827$ at the location where the pressure peaked ($\beta = 16$ mm). The particles begin to decrease in size when $\beta > Z_{CW}$ (6.77 mm).

As the particles get smaller and smaller the "characteristic" relaxation times for particle velocity and temperature reduce as the square of the particle diameter. Hence there is a rapid adjustment of the particle velocity and temperature to equilibrate to the gas values within distances that become even smaller. The integration scheme utilized could not keep up with this accelerating relaxation adjustment, and numerical instability usually set in when the particles reached 1/4 of their original diameter. Obviously the code needs to be optimized for such conditions, and this effort is planned for future work.

Figure 5 presents a comparison of the pressure profiles in the relaxation zone for two cases, one with moderate-sized particles having a typical value of the energy content, and the other with large diameter particles having a low energy content. As expected, the ignition zone is much shorter with the smaller particle size. Interestingly enough the less energetic propellant of the larger diameter particles showed a larger peak pressure, i.e. $(P_g/P_o)_{\text{peak}} = 520$. One must also remember that in this comparison the solids volume fraction was equal, at 5%. And after ignition the combustion source term for the smaller 50 $\mu$m particles is actually three times greater than for the larger 150 $\mu$m size, at a same pressure condition. In conclusion, the total structure of the relaxation zone must have a significant effect on the eventual peak pressure, because from just an analysis of the combustion rate one cannot explain the differences in the predicted peak pressures for the two cases shown in figure 5.

Nevertheless, for a propellant of fixed energy content, the predicted peak pressure *increases*, as expected, as the particle diameter decreases. This is shown in figure 6 for the two shock strengths, $M_o = 3.5$ and 2.5. (The values of the maximum pressure are given the thousands-of-psi.) Notice for the nominal shock strength of $M_o = 2.5$ the predicted peak gas pressure is fairly insensitive to particle size for $d_p > 120$ $\mu$m.

Of course the shock strength, as measured by the initial Mach number, $M_o$, has a pronounced effect on the gas pressure in the relaxation zone. Notice that $(P_g/P_o)_{\max}$ is predicted to be 1700 atm for $M_o = 4.5$, as shown in figure 7.

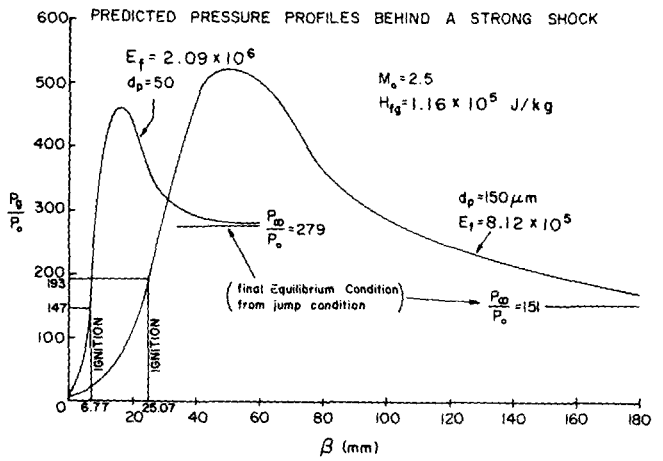


Figure 5. Predictions of the pressure distribution behind a strong shock wave for two propellants of different energy content ($d_p = 50$ $\mu$m; $M_o = 2.5$).

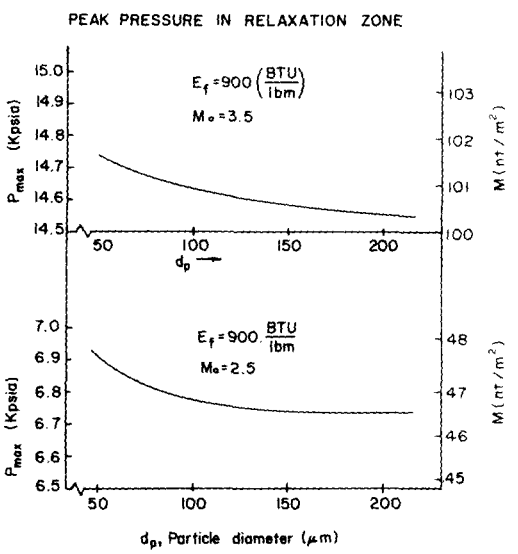


Fig. 6.

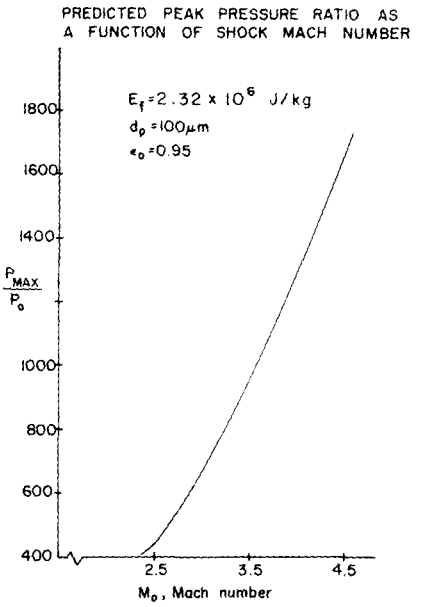


Fig. 7.

Figure 6. Peak pressure in the shock relaxation zone (for two different shock strengths) as a function of particle diameter.

Figure 7. Predicted peak pressures in the relaxation zone as a function of the shock Mach number ($d_p = 100\ \mu m$; $E_f = 2.32 \times 10^6$ J/kg ($10^3$ B.t.u./lbm)).

The relaxation zone lengths, and especially the ignition-lag distance, $Z_{CW}$, are of course strongly dependent upon the particle size, as well as the shock strength. Figure 8 presents the results of the predicted ignition-lag zone as a function of $d_p$ for two shock strengths. Notice, however, that the energy content is different for the two lines shown in figure 8.

Likewise the total relaxation zone, which here must be determined in an approximate manner by extrapolating to the distance of zero particle size, is also a strong function of the particle diameter. Figure 9 presents these results, again for two shock strengths.

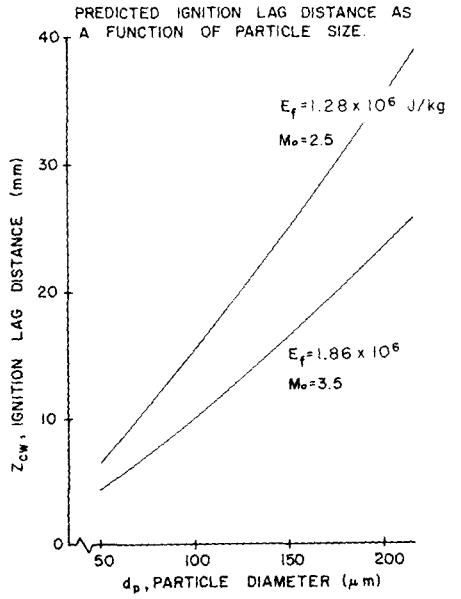


Figure 8. Predicted ignition lag distance, $Z_{CW}$, as a function of particle size for different shock strength and propellant energy content.

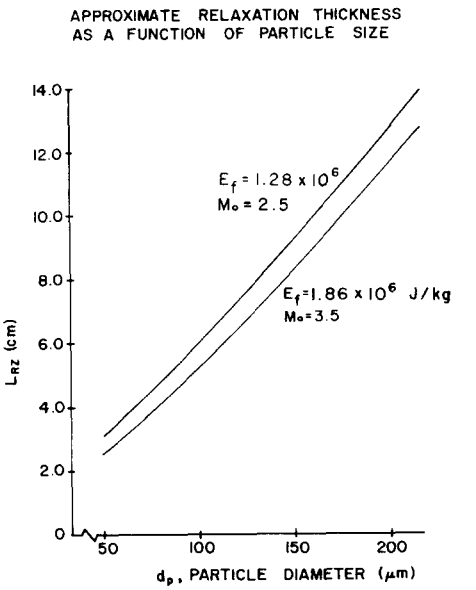


Figure 9. Approximate relaxation zone thickness, $Z_{RZ}$, as a function of particle size for two different shock strength and propellant energy content.

Several cases were studied for a "weak" shock relaxation zone condition, but because the gas temperature is not shocked to a higher value, propellant ignition is generally never predicted. Recall we assumed that the particles temperature must be raised by at least 10°C to ignite. Although the particles do heat up in a "weak" shock case, for the large mass solids loadings considered of interest here, this increase of 10° never occurred.

In order to complete the work, a case was calculated for a propellant with an assumed low ignition temperature, namely 1°C above ambient. Figure 10 shows the results. Here, $M_o = 0.90$ and $d_p = 100\ \mu$m. Eventually (after 236 mm) the particle temperature reached 296 K and burning commenced. The peak pressure ratio (not shown) was predicted to be only 14.5 atm (213 psi), although the gas temperature ratio peaked at 4.63, as shown.

A result of the type shown in figure 10 explains why the work of Kuo & Summerfield (1974, 1975), which analyzed only "weak" shocks, required an internal ignition source to raise the particle temperatures as the long ignition-lag zone developed.

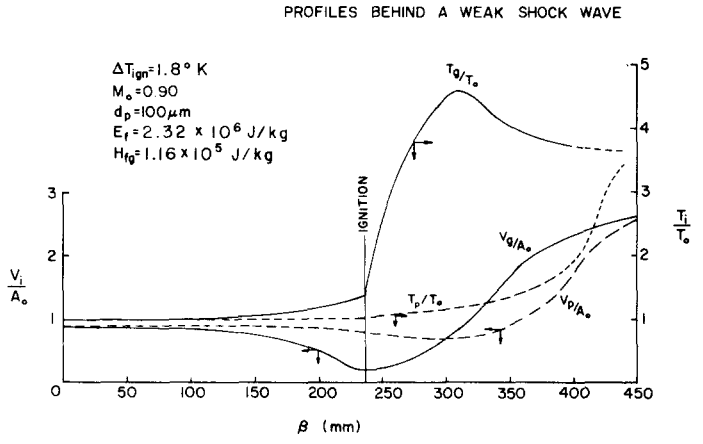


Figure 10. Predictions of the temperatures and velocities behind a "weak" shock of (reactive) propellant particles ($d_p = 100\ \mu$m; $M_o = 0.90$).

## REFERENCES

CARRIER, G. F. 1958 Shock waves in a dusty gas. *J. Fluid Mech.* **4**, 376–382.

DERR, R. L. & FLEMING, R. W. 1973 A correlation of solid propellant arc-image ignition data. *Proceedings of the 10th JANNAF Combustion Meeting*, CPIA Pub. No. 243, Vol. III, pp. 157–168.

GEAR, C. W. 1971 The automatic integration of ordinary differential equations. *Comm. ACM* **14**, 176–179; 185–190.

KRIEBEL, A. R. 1964 Analysis of normal shock waves in a particle laden gas. *J. Basic Engng* **86**, 658–663.

KRIER, H. & VAN TASSELL, W. F. 1975 Combustion and flame spreading phenomena in gas-permeable explosive materials. *Int. J. Heat Mass Transfer* **18**, 1377–1386.

KUO, K. K. & SUMMERFIELD, M. 1974 Theory of steady-state burning in gas-permeable propellants. *AIAA Jl* **12**, 49–56.

KUO, K. K. & SUMMERFIELD, M. 1975 High speed combustion of mobile granular solid propellants. *Fifteenth Symposium on Combustion*, pp. 515–527. The Combustion Institute, Pittsburgh, PA.

LU, H. Y. & CHIU, H. H. 1966 Dynamics of gases containing evaporable liquid droplets under a normal shock. *AIAA Jl* **4**, 1008–1011.

MARBLE, F. E. 1963 Dynamics of a gas containing small solid particles. *5th Colloq. Combust. Propulsion AGARD*, pp. 175–213. Pergamon Press, Oxford.

NARKIS, Y. & GAL-OR, B. 1975 Two phase flow through normal shock waves. *J. Fluid Engng* **94**, 361–365.

PANTON, R. & OPPENHEIM, A. K. 1968 Shock relaxation in a particle–gas mixture with mass transfer between phases. *AIAA Jl* **6**, 2071–2077.

RUDINGER, G. 1964 Some properties of shock relaxation in gas flows carrying small particles. *Physics Fluids* **7**, 658–663.

RUDINGER, G. 1965 Some effects of finite particle volume on the dynamics of gas–particle mixtures. *AIAA Jl* **3**, 1217–1222.

RUDINGER, G. 1969 Relaxation in gas–particle flows. *Non-Equilibrium Flows*, (Edited by WEGENER, P. P. ), pp. 119–161. Dekker, New York.

SOO, S. L. 1967 *Fluid Dynamics of Multiphase Systems*. Blaisdell, Waltham, MA.

SOO, S. L. 1976 On one-dimensional motion of a single component in two-phases. *Int. J. Heat Mass Transfer* **3**, 79–82.

## APPENDIX A

## JUMP CONDITIONS: EQUILIBRIUM VALUES AT THE END OF THE RELAXATION ZONE

The transformed, steady form of principle of conservation equations ([12]–[17]) can be integrated to give the final equilibrium properties. The Boundary Conditions discussed in the text are used as the limits of integration. By neglecting shear forces, one can easily show, for mixture continuity:

$$\int_{(o)\ddagger}^{(\infty)\dagger} \mathrm{d}\{\epsilon\rho_g v_g\} + \int_{(o)}^{(\infty)} \mathrm{d}\{(1-\epsilon)\rho_p v_p\} = 0 \qquad [A1]$$

mixture momentum:

$$\int_{(o)}^{(\infty)} \mathrm{d}\{\epsilon\rho_g v_g^2 + (1-\epsilon)\rho_p v_p^2\} = -\int_{(o)}^{(\infty)} \mathrm{d}\{P_g\} \qquad [A2]$$

†(∞) conditions at the hot end (final equilibrium).
‡(*o*) conditions at the cold end (upstream of shock).

mixture energy:

$$\int_{(o)}^{(\infty)} \mathrm{d}\{\epsilon\rho v_g e_{g_o} + (1-\epsilon)\rho_p v_p e_{p_o}\} = -\int_{(o)}^{(\infty)} \mathrm{d}P_g[\epsilon v_g + (1-\epsilon)v_p] \qquad [A3]$$

performing [A1]

$$\epsilon_{(\infty)}\rho_{g_{(\infty)}} v_g - \epsilon_{(o)}\rho_{g_{(o)}} v_{g_{(o)}} + (1-\epsilon_{(\infty)})\rho_{p_{(\infty)}} v_{p_{(\infty)}} - (1-\epsilon_{(o)})\rho_{p_{(o)}} v_{p_{(o)}} = 0 \qquad [A4]$$

simplifying:

$$\rho_\infty V_\infty = \epsilon_o \rho_{g_o} V_o + (1-\epsilon_o)\rho_p V_o \qquad [A5]$$

Likewise for mixture momentum equation [A2]:

$$\epsilon_{(\infty)}\rho_{g_{(\infty)}} v^2_{g_{(\infty)}} - \epsilon_{(o)}\rho_{g_{(o)}} v^2_{g_{(o)}} + (1-\epsilon_{(\infty)})\rho_{p_{(\infty)}} v_{p_{(\infty)}} - (1-\epsilon_{(o)})\rho_{p_{(o)}} v^2_{p_{(o)}} = -P_{(\infty)} + P_{(o)}. \qquad [A6]$$

Simplifying:

$$\rho_\infty V_\infty^2 + P_\infty = \epsilon_o \rho_{g_o} V_o^2 + (1-\epsilon_o)\rho_p V_o^2 + P_o. \qquad [A7]$$

Finally the mixture energy equation [A3] becomes

$$\begin{aligned}\epsilon_{(\infty)}\rho_{g_{(\infty)}} v_{g_{(\infty)}} (e_{g_o})_{(\infty)} - \epsilon_{(o)}\rho_{g_{(o)}} v_{g_{(o)}} (e_{g_o})_{(o)} + (1-\epsilon_{(\infty)})\rho_{p_{(\infty)}} v_{p_{(\infty)}} (e_{p_o})_{(\infty)} - (1-\epsilon_{(o)})\rho_{p_{(o)}} v_{p_{(o)}} (e_{p_o})_{(o)} \\ + \epsilon_{(\infty)} P_{g_{(\infty)}} v_{g_{(\infty)}} - \epsilon_{(o)} P_{g_{(o)}} v_{g_{(o)}} + (1-\epsilon_{(\infty)}) P_{g_{(\infty)}} v_{p_{(\infty)}} - (1-\epsilon_{(o)}) P_{g_o} v_{p_{(o)}} = 0. \end{aligned} \qquad [A8]$$

Defining

$$(e_{g_o}) = C_{v_g} T_g + \frac{1}{2} v_g^2, \qquad [A9]$$

$$(e_{p_o}) = C_p T_p + \frac{1}{2} v_p^2 + e_f. \qquad [A10]$$

Hence:

$$(e_{g_o})_{(o)} = C_{v_g} T_o + \frac{1}{2} V_o^2, \qquad [A11]$$

$$(e_{g_o})_{(\infty)} = C_{v_g} T_\infty + \frac{1}{2} V_\infty^2, \qquad [A12]$$

$$(e_{p_o})_{(o)} = C_p T_o + \frac{1}{2} V_o^2 + e_f, \qquad [A13]$$

$$(e_{p_o})_{(\infty)} = C_p T_\infty + \frac{1}{2} V_\infty^2. \qquad [A14]$$

Simplifying [A8]:

$$\rho_\infty V_\infty (e_{g_o})_{(\infty)} + P_\infty V_\infty = \epsilon_o \rho_{g_o} V_o (e_{g_o})_{(o)} + (1-\epsilon_o)\rho_p V_o (e_{p_o})_{(o)} + P_o V_o. \qquad [A15]$$

The three integrated conservation equations contain four unknowns. Thus one should combine these equations with the equation of state for the gas

$$P_\infty(\rho_\infty^{-1} - b) = \mathcal{R}_g T_\infty \qquad [A16]$$

to complete the set of four algebraic equations in four unknowns (final equilibrium properties of gas–particle mixture); $\rho_\infty$, $P_\infty$, and $T_\infty$.